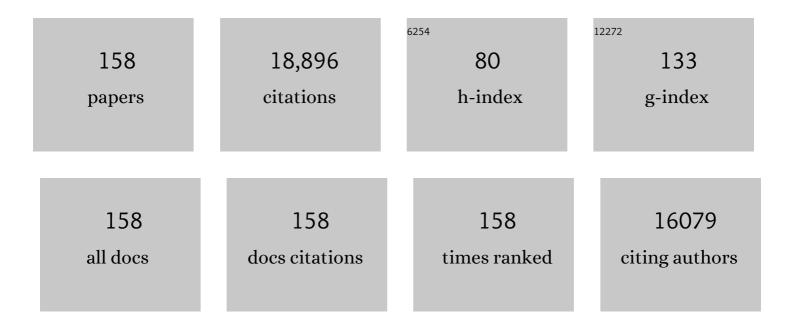
List of Publications by Year in descending order

Source: https://exaly.com/author-pdf/9277805/publications.pdf Version: 2024-02-01



#	Article	IF	CITATIONS
1	Stabilization of cadmium in contaminated sediment based on a nanoremediation strategy: Environmental impacts and mechanisms. Chemosphere, 2022, 287, 132363.	8.2	19
2	Recent progress of noble metals with tailored features in catalytic oxidation for organic pollutants degradation. Journal of Hazardous Materials, 2022, 422, 126950.	12.4	49
3	The combined toxicity and mechanism of multi-walled carbon nanotubes and nano copper oxide toward freshwater algae: Tetradesmus obliquus. Journal of Environmental Sciences, 2022, 112, 376-387.	6.1	17
4	Environmentally persistent free radicals in bismuth-based metal–organic layers derivatives: Photodegradation of pollutants and mechanism unravelling. Chemical Engineering Journal, 2022, 430, 133026.	12.7	23
5	Research progress of microplastics in soil-plant system: Ecological effects and potential risks. Science of the Total Environment, 2022, 812, 151487.	8.0	87
6	Layered double hydroxide based materials applied in persulfate based advanced oxidation processes: Property, mechanism, application and perspectives. Journal of Hazardous Materials, 2022, 424, 127612.	12.4	62
7	Biochar in the 21st century: A data-driven visualization of collaboration, frontier identification, and future trend. Science of the Total Environment, 2022, 818, 151774.	8.0	60
8	Uniform polypyrrole electrodeposition triggered by phytic acid-guided interface engineering for high energy density flexible supercapacitor. Journal of Colloid and Interface Science, 2022, 611, 356-365.	9.4	24
9	Metallic Co and crystalline Co-Mo oxides supported on graphite felt for bifunctional electrocatalytic hydrogen evolution and urea oxidation. Journal of Colloid and Interface Science, 2022, 612, 413-423.	9.4	30
10	Presence of polystyrene microplastics in Cd contaminated water promotes Cd removal by nano zero-valent iron and ryegrass (Lolium Perenne L.). Chemosphere, 2022, 303, 134729.	8.2	15
11	Cobalt Single Atoms Anchored on Oxygenâ€Doped Tubular Carbon Nitride for Efficient Peroxymonosulfate Activation: Simultaneous Coordination Structure and Morphology Modulation. Angewandte Chemie - International Edition, 2022, 61, .	13.8	97
12	Cobalt Single Atoms Anchored on Oxygenâ€Doped Tubular Carbon Nitride for Efficient Peroxymonosulfate Activation: Simultaneous Coordination Structure and Morphology Modulation. Angewandte Chemie, 2022, 134, .	2.0	25
13	Progress and challenges of metal-organic frameworks-based materials for SR-AOPs applications in water treatment. Chemosphere, 2021, 263, 127672.	8.2	138
14	Surface and interface engineering of two-dimensional bismuth-based photocatalysts for ambient molecule activation. Journal of Materials Chemistry A, 2021, 9, 196-233.	10.3	50
15	Nanoscale zerovalent iron, carbon nanotubes and biochar facilitated the phytoremediation of cadmium contaminated sediments by changing cadmium fractions, sediments properties and bacterial community structure. Ecotoxicology and Environmental Safety, 2021, 208, 111510.	6.0	45
16	Carbon Dotsâ€Decorated Carbonâ€Based Metalâ€Free Catalysts for Electrochemical Energy Storage. Small, 2021, 17, e2002998.	10.0	27
17	Topological transformation of bismuth vanadate into bismuth oxychloride: Band-gap engineering of ultrathin nanosheets with oxygen vacancies for efficient molecular oxygen activation. Chemical Engineering Journal, 2021, 420, 127573.	12.7	37
18	Microplastics and nanoplastics in the environment: Macroscopic transport and effects on creatures. Journal of Hazardous Materials, 2021, 407, 124399.	12.4	200

#	Article	IF	CITATIONS
19	Strategies for enhancing the perylene diimide photocatalytic degradation activity: method, effect factor, and mechanism. Environmental Science: Nano, 2021, 8, 602-618.	4.3	39
20	Jointed Synchronous Photocatalytic Oxidation and Chromate Reduction Enabled by the Defect Distribution upon BiVO <sub>4</sub> : Mechanism Insight and Toxicity Assessment. ACS Applied Materials & Interfaces, 2021, 13, 17586-17598.	8.0	39
21	Catalyst-free activation of permanganate under visible light irradiation for sulfamethazine degradation: Experiments and theoretical calculation. Water Research, 2021, 194, 116915.	11.3	124
22	MXenes as Superexcellent Support for Confining Single Atom: Properties, Synthesis, and Electrocatalytic Applications. Small, 2021, 17, e2007113.	10.0	52
23	Remediation of Cd-Contaminated Soil by Modified Nanoscale Zero-Valent Iron: Role of Plant Root Exudates and Inner Mechanisms. International Journal of Environmental Research and Public Health, 2021, 18, 5887.	2.6	11
24	A novel multifunctional platform based on ITO/APTES/ErGO/AuNPs for long-term cell culture and real-time biomolecule monitoring. Talanta, 2021, 228, 122232.	5.5	7
25	Visual Method for Selective Detection of Hg <sup>2+</sup> Based on the Competitive Interactions of 2-Thiobarbituric Acid with Au Nanoparticles and Hg <sup>2+</sup> . ACS Applied Nano Materials, 2021, 4, 6760-6767.	5.0	15
26	Stabilization of lead in polluted sediment based on an eco-friendly amendment strategy: Microenvironment response mechanism. Journal of Hazardous Materials, 2021, 415, 125534.	12.4	23
27	PDI Supermolecule-Encapsulated 3D BiVO <sub>4</sub> toward Unobstructed Interfacial Charge Transfer for Enhanced Visible-Light Photocatalytic Activity. Journal of Physical Chemistry C, 2021, 125, 18693-18707.	3.1	8
28	Spinel ferrites (MFe2O4): Synthesis, improvement and catalytic application in environment and energy field. Advances in Colloid and Interface Science, 2021, 294, 102486.	14.7	159
29	Phytoremediation of poly- and perfluoroalkyl substances: A review on aquatic plants, influencing factors, and phytotoxicity. Journal of Hazardous Materials, 2021, 418, 126314.	12.4	36
30	Microplastics retention by reeds in freshwater environment. Science of the Total Environment, 2021, 790, 148200.	8.0	63
31	Boron nitride quantum dots decorated MIL-100(Fe) for boosting the photo-generated charge separation in photocatalytic refractory antibiotics removal. Environmental Research, 2021, 202, 111661.	7.5	21
32	Interactions between microplastics/nanoplastics and vascular plants. Environmental Pollution, 2021, 290, 117999.	7.5	123
33	Hierarchical urchin-like amorphous carbon with Co-adding anchored on nickel foam: A free-standing electrode for advanced asymmetrical supercapacitors and adsorbed Pb (II). Journal of Colloid and Interface Science, 2021, 603, 58-69.	9.4	9
34	Oxygen vacancy-rich doped CDs@graphite felt-600 heterostructures for high-performance supercapacitor electrodes. Nanoscale, 2021, 13, 4995-5005.	5.6	15
35	Design of an amorphous and defect-rich CoMoOF layer as a pH-universal catalyst for the hydrogen evolution reaction. Journal of Materials Chemistry A, 2021, 9, 8730-8739.	10.3	38
36	Polyoxometalate@Metal–Organic Framework Composites as Effective Photocatalysts. ACS Catalysis, 2021, 11, 13374-13396.	11.2	121

#	Article	IF	CITATIONS
37	Recent development of advanced biotechnology for wastewater treatment. Critical Reviews in Biotechnology, 2020, 40, 99-118.	9.0	35
38	Distorted polymeric carbon nitride via carriers transfer bridges with superior photocatalytic activity for organic pollutants oxidation and hydrogen production under visible light. Journal of Hazardous Materials, 2020, 386, 121947.	12.4	95
39	Facet-Engineered Surface and Interface Design of Monoclinic Scheelite Bismuth Vanadate for Enhanced Photocatalytic Performance. ACS Catalysis, 2020, 10, 1024-1059.	11.2	105
40	Semiconductor-based photocatalysts for photocatalytic and photoelectrochemical water splitting: will we stop with photocorrosion?. Journal of Materials Chemistry A, 2020, 8, 2286-2322.	10.3	251
41	Recent advances in application of graphitic carbon nitride-based catalysts for degrading organic contaminants in water through advanced oxidation processes beyond photocatalysis: A critical review. Water Research, 2020, 184, 116200.	11.3	343
42	Megamerger of MOFs and g-C <sub>3</sub> N <sub>4</sub> for energy and environment applications: upgrading the framework stability and performance. Journal of Materials Chemistry A, 2020, 8, 17883-17906.	10.3	48
43	Recent advances in two-dimensional nanomaterials for photocatalytic reduction of CO <sub>2</sub> : insights into performance, theories and perspective. Journal of Materials Chemistry A, 2020, 8, 19156-19195.	10.3	101
44	Biochar-mediated Fenton-like reaction for the degradation of sulfamethazine: Role of environmentally persistent free radicals. Chemosphere, 2020, 255, 126975.	8.2	92
45	Unravelling the role of dual quantum dots cocatalyst in 0D/2D heterojunction photocatalyst for promoting photocatalytic organic pollutant degradation. Chemical Engineering Journal, 2020, 396, 125343.	12.7	132
46	Activation of persulfate by graphitized biochar for sulfamethoxazole removal: The roles of graphitic carbon structure and carbonyl group. Journal of Colloid and Interface Science, 2020, 577, 419-430.	9.4	94
47	Hybrid architectures based on noble metals and carbon-based dots nanomaterials: A review of recent progress in synthesis and applications. Chemical Engineering Journal, 2020, 399, 125743.	12.7	70
48	In Situ Grown Singleâ€Atom Cobalt on Polymeric Carbon Nitride with Bidentate Ligand for Efficient Photocatalytic Degradation of Refractory Antibiotics. Small, 2020, 16, e2001634.	10.0	235
49	A novel Fe-hemin-metal organic frameworks supported on chitosan-reduced graphene oxide for real-time monitoring of H2O2 released from living cells. Analytica Chimica Acta, 2020, 1128, 90-98.	5.4	28
50	Recent advances in conjugated microporous polymers for photocatalysis: designs, applications, and prospects. Journal of Materials Chemistry A, 2020, 8, 6434-6470.	10.3	140
51	Graphdiyne: A Rising Star of Electrocatalyst Support for Energy Conversion. Advanced Energy Materials, 2020, 10, 2000177.	19.5	100
52	Removal of Sulfamethoxazole in Aqueous Solutions by Iron-Based Advanced Oxidation Processes: Performances and Mechanisms. Water, Air, and Soil Pollution, 2020, 231, 1.	2.4	11
53	Megamerger of biosorbents and catalytic technologies for the removal of heavy metals from wastewater: Preparation, final disposal, mechanism and influencing factors. Journal of Environmental Management, 2020, 261, 109879.	7.8	60
54	Interface modulation of Mo <sub>2</sub> C@foam nickel <i>via</i> MoS <sub>2</sub> quantum dots for the electrochemical oxygen evolution reaction. Journal of Materials Chemistry A, 2020, 8, 15074-15085.	10.3	25

#	Article	IF	CITATIONS
55	Silver-based semiconductor Z-scheme photocatalytic systems for environmental purification. Journal of Hazardous Materials, 2020, 390, 122128.	12.4	122
56	Unravelling the interfacial charge migration pathway at atomic level in 2D/2D interfacial Schottky heterojunction for visible-light-driven molecular oxygen activation. Applied Catalysis B: Environmental, 2020, 266, 118650.	20.2	150
57	Sustainable hydrogen production by molybdenum carbide-based efficient photocatalysts: From properties to mechanism. Advances in Colloid and Interface Science, 2020, 279, 102144.	14.7	55
58	Strategy to improve gold nanoparticles loading efficiency on defect-free high silica ZSM-5 zeolite for the reduction of nitrophenols. Chemosphere, 2020, 256, 127083.	8.2	57
59	Degradation of sulfamethazine by biochar-supported bimetallic oxide/persulfate system in natural water: Performance and reaction mechanism. Journal of Hazardous Materials, 2020, 398, 122816.	12.4	133
60	How does the microenvironment change during the stabilization of cadmium in exogenous remediation sediment?. Journal of Hazardous Materials, 2020, 398, 122836.	12.4	21
61	Dugongs under threat. Science, 2019, 365, 552-552.	12.6	7
62	Visible-light-driven photocatalytic degradation of sulfamethazine by surface engineering of carbon nitride:Properties, degradation pathway and mechanisms. Journal of Hazardous Materials, 2019, 380, 120815.	12.4	131
63	Hierarchical porous carbon material restricted Au catalyst for highly catalytic reduction of nitroaromatics. Journal of Hazardous Materials, 2019, 380, 120864.	12.4	110
64	Chloro-phosphate impregnated biochar prepared by co-precipitation for the lead, cadmium and copper synergic scavenging from aqueous solution. Bioresource Technology, 2019, 293, 122102.	9.6	50
65	Recent advances in covalent organic frameworks (COFs) as a smart sensing material. Chemical Society Reviews, 2019, 48, 5266-5302.	38.1	630
66	Multiple charge-carrier transfer channels of Z-scheme bismuth tungstate-based photocatalyst for tetracycline degradation: Transformation pathways and mechanism. Journal of Colloid and Interface Science, 2019, 555, 770-782.	9.4	45
67	Covalent triazine frameworks for carbon dioxide capture. Journal of Materials Chemistry A, 2019, 7, 22848-22870.	10.3	106
68	Ultrathin oxygen-vacancy abundant WO3 decorated monolayer Bi2WO6 nanosheet: A 2D/2D heterojunction for the degradation of Ciprofloxacin under visible and NIR light irradiation. Journal of Colloid and Interface Science, 2019, 556, 557-567.	9.4	89
69	A fantastic two-dimensional MoS2 material based on the inert basal planes activation: Electronic structure, synthesis strategies, catalytic active sites, catalytic and electronics properties. Coordination Chemistry Reviews, 2019, 399, 213020.	18.8	101
70	Roles of multiwall carbon nanotubes in phytoremediation: cadmium uptake and oxidative burst in <i>Boehmeria nivea</i> (L.) Gaudich. Environmental Science: Nano, 2019, 6, 851-862.	4.3	34
71	Adsorption behavior of engineered carbons and carbon nanomaterials for metal endocrine disruptors: Experiments and theoretical calculation. Chemosphere, 2019, 222, 184-194.	8.2	157
72	Black Phosphorus, a Rising Star 2D Nanomaterial in the Postâ€Graphene Era: Synthesis, Properties, Modifications, and Photocatalysis Applications. Small, 2019, 15, e1804565.	10.0	244

#	Article	IF	CITATIONS
73	Degradation of naphthalene with magnetic bio-char activate hydrogen peroxide: Synergism of bio-char and Fe–Mn binary oxides. Water Research, 2019, 160, 238-248.	11.3	335
74	How do proteins â€~response' to common carbon nanomaterials?. Advances in Colloid and Interface Science, 2019, 270, 101-107.	14.7	13
75	Effects of typical engineered nanomaterials on 4-nonylphenol degradation in river sediment: based on bacterial community and function analysis. Environmental Science: Nano, 2019, 6, 2171-2184.	4.3	8
76	Peroxidaseâ€Like Activity of Smart Nanomaterials and Their Advanced Application in Colorimetric Glucose Biosensors. Small, 2019, 15, e1900133.	10.0	145
77	Decontamination of lead and tetracycline from aqueous solution by a promising carbonaceous nanocomposite: Interaction and mechanisms insight. Bioresource Technology, 2019, 283, 277-285.	9.6	98
78	Synergistic effect of artificial enzyme and 2D nano-structured Bi2WO6 for eco-friendly and efficient biomimetic photocatalysis. Applied Catalysis B: Environmental, 2019, 250, 52-62.	20.2	340
79	Fabrication of novel magnetic MnFe2O4/bio-char composite and heterogeneous photo-Fenton degradation of tetracycline in near neutral pH. Chemosphere, 2019, 224, 910-921.	8.2	287
80	Effects of multi-walled carbon nanotubes on metal transformation and natural organic matters in riverine sediment. Journal of Hazardous Materials, 2019, 374, 459-468.	12.4	27
81	Immobilized laccase on bentonite-derived mesoporous materials for removal of tetracycline. Chemosphere, 2019, 222, 865-871.	8.2	121
82	Biochar facilitated the phytoremediation of cadmium contaminated sediments: Metal behavior, plant toxicity, and microbial activity. Science of the Total Environment, 2019, 666, 1126-1133.	8.0	122
83	In-situ deposition of gold nanoparticles onto polydopamine-decorated g-C3N4 for highly efficient reduction of nitroaromatics in environmental water purification. Journal of Colloid and Interface Science, 2019, 534, 357-369.	9.4	200
84	Recent progress in covalent organic framework thin films: fabrications, applications and perspectives. Chemical Society Reviews, 2019, 48, 488-516.	38.1	564
85	Colorimetric determination of mercury(II) using gold nanoparticles and double ligand exchange. Mikrochimica Acta, 2019, 186, 31.	5.0	38
86	Immobilizing laccase on kaolinite and its application in treatment of malachite green effluent with the coexistence of Cd (ĐŸ). Chemosphere, 2019, 217, 843-850.	8.2	51
87	Cr(VI) removal from aqueous solution using biochar modified with Mg/Al-layered double hydroxide intercalated with ethylenediaminetetraacetic acid. Bioresource Technology, 2019, 276, 127-132.	9.6	191
88	Deciphering the Fenton-reaction-aid lignocellulose degradation pattern by Phanerochaete chrysosporium with ferroferric oxide nanomaterials: Enzyme secretion, straw humification and structural alteration. Bioresource Technology, 2019, 276, 335-342.	9.6	41
89	Synthetic strategies and application of gold-based nanocatalysts for nitroaromatics reduction. Science of the Total Environment, 2019, 652, 93-116.	8.0	44
90	Fabrication of CuS/BiVO4 (0â€ <sup>-</sup> 4â€ <sup>-</sup> 0) binary heterojunction photocatalysts with enhanced photocatalytic activity for Ciprofloxacin degradation and mechanism insight. Chemical Engineering Journal, 2019, 358, 891-902.	12.7	401

#	Article	IF	CITATIONS
91	Nanoscale zero-valent iron assisted phytoremediation of Pb in sediment: Impacts on metal accumulation and antioxidative system of Lolium perenne. Ecotoxicology and Environmental Safety, 2018, 153, 229-237.	6.0	118
92	Remediation of contaminated soils by enhanced nanoscale zero valent iron. Environmental Research, 2018, 163, 217-227.	7.5	181
93	Rational Design of Carbon-Doped Carbon Nitride/Bi <sub>12</sub> O <sub>17</sub> Cl <sub>2</sub> Composites: A Promising Candidate Photocatalyst for Boosting Visible-Light-Driven Photocatalytic Degradation of Tetracycline. ACS Sustainable Chemistry and Engineering, 2018, 6, 6941-6949.	6.7	196
94	A novel biosorbent prepared by immobilized Bacillus licheniformis for lead removal from wastewater. Chemosphere, 2018, 200, 173-179.	8.2	81
95	"Gold rush―in modern science: Fabrication strategies and typical advanced applications of gold nanoparticles in sensing. Coordination Chemistry Reviews, 2018, 359, 1-31.	18.8	261
96	Cadmium immobilization in river sediment using stabilized nanoscale zero-valent iron with enhanced transport by polysaccharide coating. Journal of Environmental Management, 2018, 210, 191-200.	7.8	77
97	In Situ Grown Agl/Bi <sub>12</sub> O <sub>17</sub> Cl <sub>2</sub> Heterojunction Photocatalysts for Visible Light Degradation of Sulfamethazine: Efficiency, Pathway, and Mechanism. ACS Sustainable Chemistry and Engineering, 2018, 6, 4174-4184.	6.7	249
98	Preparation of water-compatible molecularly imprinted thiol-functionalized activated titanium dioxide: Selective adsorption and efficient photodegradation of 2, 4-dinitrophenol in aqueous solution. Journal of Hazardous Materials, 2018, 346, 113-123.	12.4	146
99	Remediation of lead-contaminated sediment by biochar-supported nano-chlorapatite: Accompanied with the change of available phosphorus and organic matters. Journal of Hazardous Materials, 2018, 348, 109-116.	12.4	128
100	High adsorption of methylene blue by salicylic acid–methanol modified steel converter slag and evaluation of its mechanism. Journal of Colloid and Interface Science, 2018, 515, 232-239.	9.4	96
101	Pyrolysis and reutilization of plant residues after phytoremediation of heavy metals contaminated sediments: For heavy metals stabilization and dye adsorption. Bioresource Technology, 2018, 253, 64-71.	9.6	214
102	BiOX (X = Cl, Br, I) photocatalytic nanomaterials: Applications for fuels and environmental management. Advances in Colloid and Interface Science, 2018, 254, 76-93.	14.7	422
103	Efficient degradation of sulfamethazine in simulated and real wastewater at slightly basic pH values using Co-SAM-SCS /H2O2 Fenton-like system. Water Research, 2018, 138, 7-18.	11.3	198
104	Tween 80 surfactant-enhanced bioremediation: toward a solution to the soil contamination by hydrophobic organic compounds. Critical Reviews in Biotechnology, 2018, 38, 17-30.	9.0	80
105	Nanoscale zero-valent iron coated with rhamnolipid as an effective stabilizer for immobilization of Cd and Pb in river sediments. Journal of Hazardous Materials, 2018, 341, 381-389.	12.4	248
106	White rot fungi and advanced combined biotechnology with nanomaterials: promising tools for endocrine-disrupting compounds biotransformation. Critical Reviews in Biotechnology, 2018, 38, 671-689.	9.0	54
107	Rhamnolipid stabilized nano-chlorapatite: Synthesis and enhancement effect on Pb-and Cd-immobilization in polluted sediment. Journal of Hazardous Materials, 2018, 343, 332-339.	12.4	139
108	Highly porous carbon nitride by supramolecular preassembly of monomers for photocatalytic removal of sulfamethazine under visible light driven. Applied Catalysis B: Environmental, 2018, 220, 202-210.	20.2	478

#	Article	IF	CITATIONS
109	Remediation of contaminated soils by biotechnology with nanomaterials: bio-behavior, applications, and perspectives. Critical Reviews in Biotechnology, 2018, 38, 455-468.	9.0	158
110	Enhanced bioremediation of 4-nonylphenol and cadmium co-contaminated sediment by composting with Phanerochaete chrysosporium inocula. Bioresource Technology, 2018, 250, 625-634.	9.6	40
111	Transcriptome analysis reveals novel insights into the response to Pb exposure in Phanerochaete chrysosporium. Chemosphere, 2018, 194, 657-665.	8.2	12
112	Electrochemical Aptasensor Based on Sulfur–Nitrogen Codoped Ordered Mesoporous Carbon and Thymine–Hg <sup>2+</sup> –Thymine Mismatch Structure for Hg <sup>2+</sup> Detection. ACS Sensors, 2018, 3, 2566-2573.	7.8	137
113	Alkali Metal-Assisted Synthesis of Graphite Carbon Nitride with Tunable Band-Gap for Enhanced Visible-Light-Driven Photocatalytic Performance. ACS Sustainable Chemistry and Engineering, 2018, 6, 15503-15516.	6.7	188
114	Microplastic pollution in surface sediments of urban water areas in Changsha, China: Abundance, composition, surface textures. Marine Pollution Bulletin, 2018, 136, 414-423.	5.0	183
115	Recent advances in sensors for tetracycline antibiotics and their applications. TrAC - Trends in Analytical Chemistry, 2018, 109, 260-274.	11.4	190
116	Graphitic Carbon Nitride-Based Heterojunction Photoactive Nanocomposites: Applications and Mechanism Insight. ACS Applied Materials & Interfaces, 2018, 10, 21035-21055.	8.0	266
117	Facile Hydrothermal Synthesis of <i>Z</i> -Scheme Bi <sub>2</sub> Fe <sub>4</sub> O <sub>9</sub> /Bi <sub>2</sub> WO <sub>6</sub> Heterojunction Photocatalyst with Enhanced Visible Light Photocatalytic Activity. ACS Applied Materials & Interfaces. 2018. 10. 18824-18836.	8.0	397
118	Responses of microbial carbon metabolism and function diversity induced by complex fungal enzymes in lignocellulosic waste composting. Science of the Total Environment, 2018, 643, 539-547.	8.0	24
119	Nanoremediation of cadmium contaminated river sediments: Microbial response and organic carbon changes. Journal of Hazardous Materials, 2018, 359, 290-299.	12.4	110
120	Performance and toxicity assessment of nanoscale zero valent iron particles in the remediation of contaminated soil: A review. Chemosphere, 2018, 210, 1145-1156.	8.2	149
121	Difunctional chitosan-stabilized Fe/Cu bimetallic nanoparticles for removal of hexavalent chromium wastewater. Science of the Total Environment, 2018, 644, 1181-1189.	8.0	76
122	Chromosomal expression of CadR on Pseudomonas aeruginosa for the removal of Cd(II) from aqueous solutions. Science of the Total Environment, 2018, 636, 1355-1361.	8.0	64
123	A visual application of gold nanoparticles: Simple, reliable and sensitive detection of kanamycin based on hydrogen-bonding recognition. Sensors and Actuators B: Chemical, 2017, 243, 946-954.	7.8	170
124	The effects of rice straw biochar on indigenous microbial community and enzymes activity in heavy metal-contaminated sediment. Chemosphere, 2017, 174, 545-553.	8.2	267
125	The rapid degradation of bisphenol A induced by the response of indigenous bacterial communities in sediment. Applied Microbiology and Biotechnology, 2017, 101, 3919-3928.	3.6	34
126	Effects of calcium at toxic concentrations of cadmium in plants. Planta, 2017, 245, 863-873.	3.2	169

#	Article	IF	CITATIONS
127	Titanium dioxide nanotube arrays with silane coupling agent modification for heavy metal reduction and persistent organic pollutant degradation. New Journal of Chemistry, 2017, 41, 4377-4389.	2.8	22
128	Chitosan-wrapped gold nanoparticles for hydrogen-bonding recognition and colorimetric determination of the antibiotic kanamycin. Mikrochimica Acta, 2017, 184, 2097-2105.	5.0	79
129	Precipitation, adsorption and rhizosphere effect: The mechanisms for Phosphate-induced Pb immobilization in soils—A review. Journal of Hazardous Materials, 2017, 339, 354-367.	12.4	327
130	Lead-induced oxidative stress and antioxidant response provide insight into the tolerance of Phanerochaete chrysosporium to lead exposure. Chemosphere, 2017, 187, 70-77.	8.2	58
131	Stabilized Nanoscale Zerovalent Iron Mediated Cadmium Accumulation and Oxidative Damage of <i>Boehmeria nivea</i> (L.) Gaudich Cultivated in Cadmium Contaminated Sediments. Environmental Science & Technology, 2017, 51, 11308-11316.	10.0	248
132	Sorptive removal of ionizable antibiotic sulfamethazine from aqueous solution by graphene oxide-coated biochar nanocomposites: Influencing factors and mechanism. Chemosphere, 2017, 186, 414-421.	8.2	158
133	Effect of Phanerochaete chrysosporium inoculation on bacterial community and metal stabilization in lead-contaminated agricultural waste composting. Bioresource Technology, 2017, 243, 294-303.	9.6	121
134	Spatiotemporal and species variations in prokaryotic communities associated with sediments from surface-flow constructed wetlands for treating swine wastewater. Chemosphere, 2017, 185, 1-10.	8.2	19
135	Synthesis and application of magnetic chlorapatite nanoparticles for zinc (II), cadmium (II) and lead (II) removal from water solutions. Journal of Colloid and Interface Science, 2017, 505, 824-835.	9.4	43
136	Manganese-enhanced degradation of lignocellulosic waste by Phanerochaete chrysosporium: evidence of enzyme activity and gene transcription. Applied Microbiology and Biotechnology, 2017, 101, 6541-6549.	3.6	21
137	Incentive effect of bentonite and concrete admixtures on stabilization/solidification for heavy metal-polluted sediments of Xiangjiang River. Environmental Science and Pollution Research, 2017, 24, 892-901.	5.3	20
138	Combination of Fenton processes and biotreatment for wastewater treatment and soil remediation. Science of the Total Environment, 2017, 574, 1599-1610.	8.0	282
139	Practical and regenerable electrochemical aptasensor based on nanoporous gold and thymine-Hg 2+ -thymine base pairs for Hg 2+ detection. Biosensors and Bioelectronics, 2017, 90, 542-548.	10.1	98
140	Degradation of atrazine by a novel Fenton-like process and assessment the influence on the treated soil. Journal of Hazardous Materials, 2016, 312, 184-191.	12.4	168
141	Synthesis and evaluation of a new class of stabilized nano-chlorapatite for Pb immobilization in sediment. Journal of Hazardous Materials, 2016, 320, 278-288.	12.4	118
142	Immobilization of Cd in river sediments by sodium alginate modified nanoscale zero-valent iron: Impact on enzyme activities and microbial community diversity. Water Research, 2016, 106, 15-25.	11.3	241
143	Influence of morphological and chemical features of biochar on hydrogen peroxide activation: implications on sulfamethazine degradation. RSC Advances, 2016, 6, 73186-73196.	3.6	98
144	Composting of 4-nonylphenol-contaminated river sediment with inocula of Phanerochaete chrysosporium. Bioresource Technology, 2016, 221, 47-54.	9.6	40

#	Article	IF	CITATIONS
145	åœŸæ›²éœ‰æ¥æ°çš"β-è'¡è"糖苷酶的酶å¦ç‰¹æ€§åŠå…¶å⁻¹å§è±†å¼,黄酮的水解. Journal of Zheji	an2g8Unive	erstag: Scienc
146	Effects of exogenous calcium and spermidine on cadmium stress moderation and metal accumulation in Boehmeria nivea (L.) Gaudich. Environmental Science and Pollution Research, 2016, 23, 8699-8708.	5.3	54
147	Efficacy of carbonaceous nanocomposites for sorbing ionizable antibiotic sulfamethazine from aqueous solution. Water Research, 2016, 95, 103-112.	11.3	326
148	Nanoporous Au-based chronocoulometric aptasensor for amplified detection of Pb2+ using DNAzyme modified with Au nanoparticles. Biosensors and Bioelectronics, 2016, 81, 61-67.	10.1	126
149	Sensitive and selective detection of mercury ions based on papain and 2,6-pyridinedicarboxylic acid functionalized gold nanoparticles. RSC Advances, 2016, 6, 3259-3266.	3.6	33
150	Bioremediation of soils contaminated with polycyclic aromatic hydrocarbons, petroleum, pesticides, chlorophenols and heavy metals by composting: Applications, microbes and future research needs. Biotechnology Advances, 2015, 33, 745-755.	11.7	706
151	Study of the degradation of methylene blue by semi-solid-state fermentation of agricultural residues with Phanerochaete chrysosporium and reutilization of fermented residues. Waste Management, 2015, 38, 424-430.	7.4	50
152	Growth, metabolism of Phanerochaete chrysosporium and route of lignin degradation in response to cadmium stress in solid-state fermentation. Chemosphere, 2015, 138, 560-567.	8.2	30
153	Influence of exogenous lead pollution on enzyme activities and organic matter degradation in the surface of river sediment. Environmental Science and Pollution Research, 2015, 22, 11422-11435.	5.3	19
154	Bioconversion of oxygen-pretreated Kraft lignin to microbial lipid with oleaginous Rhodococcus opacus DSM 1069. Green Chemistry, 2015, 17, 2784-2789.	9.0	117
155	Combined removal of di(2-ethylhexyl)phthalate (DEHP) and Pb( <scp>ii</scp> ) by using a cutinase loaded nanoporous gold-polyethyleneimine adsorbent. RSC Advances, 2014, 4, 55511-55518.	3.6	47
156	Photocatalytic degradation of phenol by the heterogeneous Fe <sub>3</sub> O <sub>4</sub> nanoparticles and oxalate complex system. RSC Advances, 2014, 4, 40828-40836.	3.6	27
157	Antioxidant activity of carboxymethyl (1→3)-β-d-glucan (from the sclerotium of Poria cocos) sulfate (in) Tj ETQq	1 <u>1</u> 0.784 7.5	314 rgBT /0
158	Functionalized Gold Nanoparticles for Visual Determination of Dopamine in Biological Fluids. ACS Applied Nano Materials, 0, , .	5.0	4